Surface particle detection for the 0.07 μm generation and beyond

Benjamin D. Buckner[a], Lakkapragada Suresh[b], and E. Dan Hirleman[c]

Department of Mechanical and Aerospace Engineering, Arizona State University

ABSTRACT

The detection of surface particles has become important in contamination control over the years. However, the minimum particle size required to be detected has been becoming smaller as IC geometries shrink. Current visible-light detection systems can detect particles down to around 60 nm in polystyrene-latex-equivalent size and so should be adequate for geometries down to around 0.18 μm, but a quick glance at the National Technology Roadmap for Semiconductors shows that geometries are expected to become as small as 0.07 μm in a little over ten years, requiring the ability to detect particles around 20 nm in diameter. This is beyond the capability of current visible-light scanners, so the Semiconductor Research Corporation has recently commissioned our group to conduct research into the limits of optical defect detection and potential of alternative detection technologies. This research centers on short-wavelength optical systems and scanned electron-beam systems as the most likely candidate technologies for high-speed nanoparticle detection. In this paper we develop a model for the analysis of the performance of hypothetical short-wavelength surface inspection systems and examine the manifold difficulties involved with using those wavelengths. The properties of scattering in the transitional region between the UV and X-ray regimes are also examined.

Keywords: surface inspection, defect detection, nanoparticles, ultraviolet light scattering, X-ray scattering

1. INTRODUCTION

The detection of surface particles has become important in contamination control over the years. However, the minimum particle size required to be detected has been becoming smaller as the size of integrated circuit patterns shrinks. A widely applied rule-of-thumb for the smallest particle of interest is a particle with a diameter nearly 1/3 the line width, though this ratio does vary somewhat with application. Current visible-light detection systems can detect particles down to around 60 nm in PSL-equivalent size, and so are adequate for geometries down to 0.18 μm. Unfortunately, a quick glance at the National Technology Roadmap for Semiconductors[1] (NTRS) will show that geometries are expected to become as small as 0.07 μm in the next ten years, requiring the ability to detect particles around 20 nm in diameter. This is far beyond the capability of current visible-light scanners, considering that the particle scattering cross section from sub-wavelength-size particles tends to fall off as something like the 6th power of diameter.

It is generally expected that detection of these smaller nanoparticles can be achieved by reducing the wavelength of illumination used by the scanner. In the case of particles much smaller than the illuminating wavelength such as we have here, while scattering cross-section tends to decrease rapidly with diameter, the cross-section also increases rapidly as the wavelength decreases. It is this fact which holds out hope that short-wavelength optical systems can provide the required sensitivity to nanoparticles.

The purpose of the present work is to examine whether this hope is truly justified and, if so, what wavelengths will be necessary and what complications will be encountered as the illumination wavelength shrinks to keep pace with the required detection limit.

2. ULTIMATE LIMITATIONS IMPOSED BY HIGH-SPEED SCANNING

Defect detection is an inherently probabilistic process. Because of the high scan-speeds needed, only a small amount of illumination reaches a specific defect and so the received amount of scattered light from the defect tends to be quite small.

[a] Email: ben.buckner@asu.edu; WWW: http://enws347.eas.asu.edu; Telephone (602) 965-3274
[b] Email: suresh@enws347.eas.asu.edu
[c] Email: hirleman@asu.edu

This means that the quantization of light into photons becomes quite prominent and introduces a significant element of shot noise. Furthermore, a background signal always exists in the form of stray light, electronic noise, detector dark current, and even roughness-originated surface-scatter for some cases.

Because of this background noise some sort of discrimination is used to distinguish random fluctuations in the background signal from small fluctuations due to a defect signal. Requirements for current scanners demand an extremely low likelihood of miscounting a background fluctuation as a defect, (a *false count*), typically on the order of 10 per wafer. This requires a very tight criterion for indicating a defect, but such a criterion also tends to make it likely that many small defect signals will be rejected as noise. Typically scanners are required to detect 90% or 95% of a type of defect in order for it to be considered detectable. Some terminology also distinguishes as *nuisance counts* those counts due to *localized light scatterers* which are not of interest in the particular application or due to noise fluctuations in combination with them.. In typical particle-detection applications, nuisance counts can be due to even smaller particles or so-called *crystal-originated particles* (COPs), various crystal imperfections including defects in the substrate, defects in underlying films, and surface defects, which are only somewhat vaguely distinguished from surface roughness.

The consequence of this extremely tight detection criterion is that a fairly significant number of additional photons must be produced above the background in order for us to be able to detect defects reliably without getting an unacceptably large number of false counts. In order to determine whether a particle or other defect can be detected we need to find out how many photons are required to constitute the defect signal in order for the signal to be distinguished from a given background.

In this work, the particular defects of interest are surface particles, but much of what applies to particle detection applies to defect detection in general. The main difference in the more general case is that the effect of scattering by a defect is not necessarily to add to the received signal, as, for example, a defect on a patterned wafer. This complication makes the general case somewhat more difficult to analyze, though the same basic concepts still apply. It should be noted that bright-field (or light-channel) scatterometry has the same complication, though in that case the complication can be dealt with easily.

We begin by breaking the scanning process down into discrete rectangular sampling regions that tile the surface. As an approximation we can consider these to be rectangular, although the beam footprint is obviously more elliptical and additionally the beam usually has a roughly Gaussian irradiance profile. These two properties can actually have subtle effects on the detection and false count probabilities, but for this rough analysis we can reasonably treat the sampling regions as having width and length equal to the corresponding $1/e^2$ axis-lengths of the elliptical beam footprint. Also, much of the possible loss in detection probability due to the beam's Gaussian profile can be compensated for by special detection schemes so it will be assumed that the somewhat optimistic estimates obtained from this flat, rectangular approximate beam with a simple detection scheme could in fact be approached in practice.

Thus we begin analyzing this problem in terms of the classic binary detection problem with a simple single threshold. We pick an appropriate threshold signal level $\eth$ (based on the allowed false count probability P_f as per the Neyman-Pearson test), and signals less than $\eth$ are rejected while signals greater than $\eth$ are accepted as particle counts. While it is well-known that in fact a Maximum Likelihood (ML) ratio test performs better than a simple threshold, for this application it is readily seen that the ML test is for all practical purposes the same as a simple threshold test.

It is important to realize however, that even if the background were perfectly dark such that any signal over zero could be considered a particle, shot noise would still prevent any particle which produces a signal with less than a certain mean flux from being detected.

For a deterministic (non-random) mean flux, the arrival of photons at the detector is described well by a Poisson random process. To analyze the influence of background on the detection limit, we need to use the properties of this process. To begin, we take the expression for the probability of a certain number of photons i to arrive during a sampling period with a mean number m of photons arriving over that period, the Poisson-distribution probability mass function (PMF)

$$\mathrm{f}(i,m) = \frac{e^{-m} m^{i}}{i!}, i \geq 0, m \geq 0. \qquad (1)$$

The probability for a number of photons less than or equal to i to arrive is given by the cumulative distribution function (CDF)

$$\mathrm{F}(i,m) = \sum_{j=0}^{i} \mathrm{f}(j,m) = \sum_{j=0}^{i} \frac{e^{-m} m^{j}}{j!} \,. \tag{2}$$

We can also define a complementary CDF

$$\mathrm{Q}(i,m) = 1 - \mathrm{F}(i,m) = \sum_{j=i+1}^{\infty} \mathrm{f}(j,m) \tag{3}$$

and the inverse thereof

$$\mathrm{Q}^{-1}(p,m) = i : \mathrm{Q}(i,m) = p \tag{4}$$

(which really only exists for certain values of p, since this is a discrete distribution).

We then need to write the expression for the threshold $\eth$ which will give the required false count probability P_{F} given a mean background count per sample, C_{B},

$$\eth = \mathrm{Q}^{-1}(P_{\mathrm{F}}, C_{\mathrm{B}}) \tag{5}$$

and the expression for detection probability P_{D} given a threshold $\eth$ and a mean particle signal count C_{S},

$$P_{\mathrm{D}} = \mathrm{Q}(t, C_{\mathrm{S}}) = \mathrm{Q}(\mathrm{Q}^{-1}(P_{\mathrm{F}}, C_{\mathrm{B}}), C_{\mathrm{S}}) \,. \tag{6}$$

Of course, what we now want to know is how much signal count C_{S} is required to meet our minimum requirement on P_{D}, so we need to invert Q(i,m) with respect to m rather than i. While functions f, F, F^{-1}, and Q ($\mathrm{Q}^{-1}(p,m)$ is simply obtained from $\mathrm{F}^{-1}(1\text{-}p,m)$) are readily available in most mathematics function libraries, the inverse of Q(i,m) for m is not, though it is fairly easy to write such a function. The only difficulty comes with large values of C_{S} and C_{B}, for which the factorial divisor in the PMF can present difficulties and the discrete summation becomes very time consuming and inaccurate due to the large number of terms. For these values, it is best to approximate the Poisson distribution with the normal distribution N(m, m), to which it tends for large mean parameters. It should be noted though, that the exact Poisson distribution is necessary to describe the situation accurately when C_{S} and C_{B} are small, which is often the case since it is desirable to have the detection system operating at as high a speed as possible.

We shall call this special inverse function $\mathrm{Q}_{\mathrm{m}}^{-1}(i, p)$ so that

$$C_{\mathrm{S}} = \mathrm{Q}_{m}^{-1}(\eth, P_{\mathrm{D}}) = \mathrm{Q}_{m}^{-1}(\mathrm{Q}^{-1}(P_{\mathrm{F}}, C_{\mathrm{B}}), P_{\mathrm{D}}) \tag{7}$$

gives us the required particle signal mean count for detection with a mean background count of C_{B}, the allowable false count probability set to P_{F}, and a required detection probability of P_{D}.

If we set the background to 0, $\eth$ is 0 as well, since any detected photons would then have to indicate a particle. From the previous development,

$$C_{\mathrm{S}} = \mathrm{Q}_{m}^{-1}(0, 0.95) = 3 \tag{8}$$

so we see that a mean of 3 photons per sample is required in order for there to be a 95% chance that at least one photon is observed in a sample where a particle is present. Since this is a best-case scenario (a noiseless, dark background) at least a three-photon mean signal count is always required to achieve 95% probability of detection. 95% is, incidentally, a convenient choice as a detection probability because it happens to be the exact probability for Q(0,3).

Setting a value for P_f, the false-count probability, in terms of the common 10-count-per-wafer specification requires figuring the number of samples per wafer. If we start by assuming a relatively small (for optical beams) 5 µm × 5 µm sample area and a 300 mm wafer we find that the number of samples N_S is around 3E9, of which 10 can be false counts. This gives us a P_f = 1-1/3E8, around 0.999999999. Computing the threshold required to get a probability so close to one is somewhat tricky to do, but it can be done with sufficiently high accuracy in the floating-point representation. Making the beam smaller yields a corresponding increase in number of 9s at the end of the decimal expression and in the required threshold while increasing the beam size decreases the number of 9s and reduces the required threshold. For a probability so near to unity, though, the threshold does not change very quickly with beam size. Figure 1 shows the required mean signal count (particle signal plus any background) *vs.* mean background count computed via eqn. (7) for several P_f values on a log-log plot. Note that the plot approaches a straight line for large means, in which region the distribution can be approximated by the normal, as mentioned earlier.

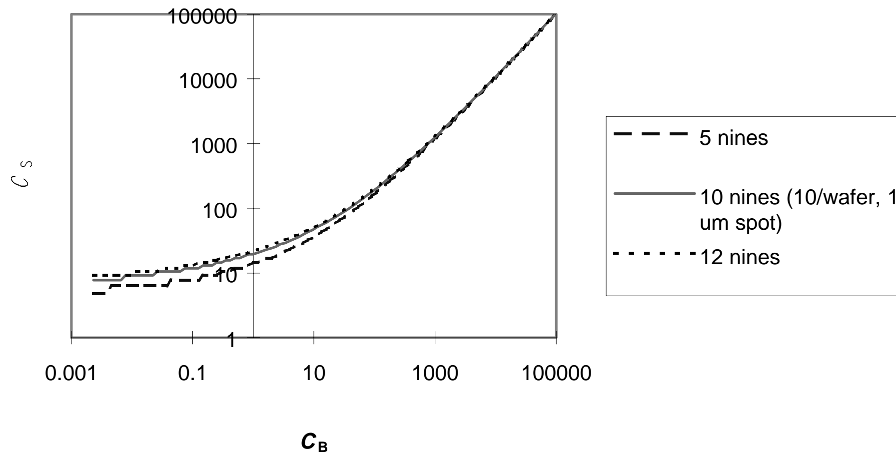

Figure 1. Mean Signal Count vs. Mean Background Count

This computation enables us to determine how much scattering a particle must produce to be detectable against a given background.

There is a certain subtle point which needs to be addressed concerning C_S though. C_S is the **total** mean signal count, inclusive of any background detected along with the particle signal C_P. The extent to which C_P and C_S differ depends to a large degree on the type of system involved. They are approximately the same if $C_P >> C_B$ or if the system involves a great deal of "shadowing" by the particle, which is to say that the presence of the particle reduces the background signal by some means. In general, shadowing is not a significant effect in optical systems, though it could be in other types of systems and in certain somewhat exotic optical detection schemes. Consequently, the C_S here should really thought of as the sum of the particle scatter (or other intensity-additive effect) and the background or the background reduced by a certain amount to account for non-negligible partial shadowing. All further such plots in this paper are of C_P *vs.* C_B since shadowing is assumed to be negligible.

It should also be restated that this analysis assumes deterministic values for C_S and C_B. Analyses accounting for random C_S and C_B have been performed for visible-wavelength optical systems,[2] and the results can be quite useful in understanding what factors influence high-speed detection performance. This analysis, though, can also be quite complicated, often requiring extensive numerical calculations and certainly requiring estimates of a number of system parameters which are not readily determined for the as-yet hypothetical systems in question here.

Even determining the background expected in a hypothetical instrument is rather difficult. As mentioned, rough surfaces can potentially contribute a significant amount of background which does tend to increase as wavelength decreases (for RMS roughness less than the wavelength), albeit at a somewhat slower rate than that often seen with particle scatter.

Figure 2 shows a plot of the mean particle signal count per sample (C_P) *versus* roughness-originated background count, calculated for a hypothetical whole-hemisphere-integrating ultraviolet system. An unrealistically low RMS roughness of 0.1 nm (1 Å) was assumed, using a scalar roughness scattering model by Elson *et al*.[3] This model assumes RMS roughness much less than the wavelength and long lateral correlation lengths, which are usual in bare silicon wafers, and it assumes no shadowing. Signals from scattering by several PSL particle sizes and several wavelengths are shown, as simulated with DDSURF.[4]

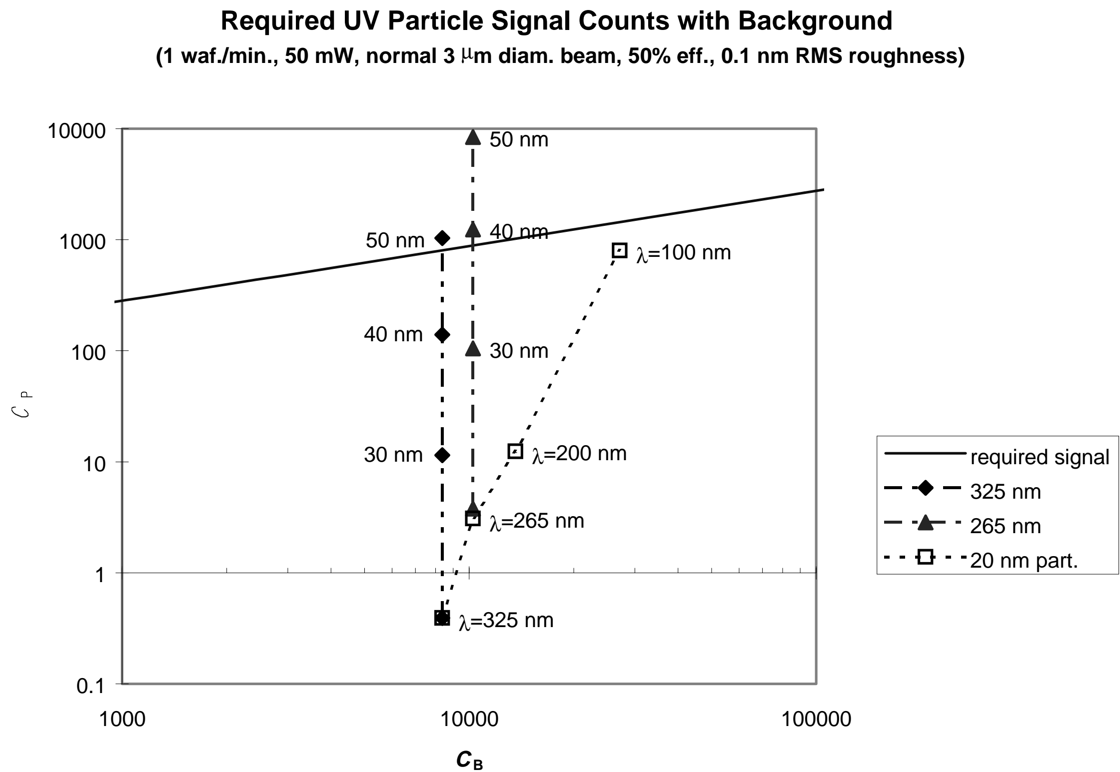

Figure 2. Required signal *vs.* background signal for an ultraviolet TIS system. The calculations were performed for polystyrene latex particle on silicon wafer, with RMS roughness of 0.1 nm.

The solid indicates the minimum detectable mean signal for the background (from eqn. (7)) for P_f = 0.999999999 and P_D = 0.95.

Of course, the surfaces of unpatterned wafers do tend to be quite smooth, with RMS roughness less than 1 nm in magnitude and extremely long lateral correlation lengths. Additionally, the use of polarization, selected incidence angles, and angle-resolved filtering can significantly reduce the influence of roughness. This usually makes roughness insignificant in the case of unpatterned wafers. Therefore we must look to other background sources for them.

One of the background sources of greatest concern as wavelengths shorten is scattering by the ambient. This scattering in a normal atmosphere has two main components which must be distinguished, particulates and spontaneous density fluctuations. Particulate scattering is due to contaminant particles much larger than the molecules, often even larger than the illuminating wavelength in untreated atmosphere. For the sub-wavelength particulates (Rayleigh scattering), scattering increases in cross-section as the 4th power of illuminating frequency so that even just halving the wavelength yields

a factor of 16 increase. Wavelength-scale and super-wavelength-scale particulates tend to scatter independent of wavelength. [5]

Spontaneous density fluctuations are quite different. To think of them in terms of solid-state physics, these are analogous to transient "dislocations" in the gas associated with the fast random motion of the molecules of the ambient. This scattering increases linearly as the pressure (or, more fundamentally, number density) increases, so its influence can be controlled by reducing the ambient pressure.

Of course, particle detection occurs in a clean environment anyway, so the particulate issue is not significant in this application, but it is already coming to be recognized that Rayleigh scattering, apparently due in this case to the fluctuation mechanism almost entirely, is one of the most significant issues in shorter-wavelength scanning systems.

To model the effects of fluctuation scattering, we need information about the optical path length in the instrument as well as information about the instrument's ability to reject stray light as well as the general geometry of the system.

The convergence of the beam does not really affect the total Rayleigh scattering because the increased intensity as it focuses is offset by the decreased number of molecules in the beam. Because of this, only the path length needs to be specified. Figuring the effective path length can be difficult, however. This is the length of the path through which the light scattered in incident and specular beams can be collected or fall into the collector's field of view. This length will strongly depend on many details of the instrument's design, and may be governed by a tradeoff between decreasing stray light and increasing the solid angle for collecting particle scatter. A generic value of 100 μm has been chosen partly because it seems to be optically attainable and partly because it comes close to predicting the rough point at which Rayleigh scatter seems to become significant in longer wavelength systems.

From Penndorf[6] we can get the Rayleigh volume scattering coefficient β at various wavelengths.

Wavelength (nm)	β (cm^{-1})	length (cm)	Rayleigh scatt. pow.	20 nm scatt. Pow.
325	1.08E-06	0.01	1.08E-08	6.30446E-11
265	2.62E-06	0.01	2.62E-08	6.10318E-10
200	9.54E-06	0.01	9.54E-08	3.24204E-09
				60 nm scatt. Pow.
488 (β @ 490)	1.97E-07	0.01	1.97E-09	2.00E-08

Table 1. Total integrated scatter (TIS) of beam with unit power by 100 μm of standard atmosphere compared to scatter by PSL particles on silicon.

The approximate point at which a system will have difficulty detecting the a particle at high speed due to shot-noise effects will be in the region where the background light detected has about the same power level as the signal, though the exact can vary by orders of magnitude depending on various parameters. For small signal powers, an even higher signal-to-background ratio is needed.

A 488 nm system such as that at the bottom of the table is believed to be limited by Rayleigh scatter, so this probably presents an overestimate of the signal collected (to be expected with a TIS cross-section) and perhaps a slight underestimate of the Rayleigh contribution.

However, by looking at the table and comparing the 60 nm particle case to the 20 nm particle cases it is clear that for the smaller particles, the Rayleigh limitation must be overwhelming, even though the particle scatter does decrease faster than the Rayleigh scatter as the wavelengths decrease.

The implication of this is that 20 or 30 nm particle detection probably will not be possible by optical means without reduction of Rayleigh scatter. There are several obvious means for this, fortunately. A helium ambient at atmospheric pressure could provide nearly a 10-fold reduction, though this would probably not be sufficient. The scatter should also be linearly related to the pressure, so a simple pressure reduction in an air ambient would also suffice. The required pressure would depend on a number of variables, but we can see from the table that it would probably be lower than 10 Torr, though not so low as 1 millitorr in any case. Such a relatively modest pressure reduction does not appear to be an insurmountable challenge by any means, so it is probably safe to assume that any optical nanoparticle detection system of the future will be engineered to eliminate Rayleigh scattering from the ambient as a seriously limiting background light source.

Other stray light sources are even less easily quantifiable than Rayleigh scattering by the ambient. Rayleigh scattering occurs in lenses as well, and there is always some degree of scattered reflection off of components within the system.

It is thus unclear what the background limitation will be once the Rayleigh scattering by the ambient is removed. Ultimately the detector itself has an electronic background level which would dominate if all the optical background sources were to be eliminated, but this also depends greatly on the detector. This type of background also usually has significant random noise upon which the shot noise effect is superimposed, further complicating the analysis. The high bandwidths involved generally tend to result in large noise-equivalent-powers (NEP), so that the deviations in such underlying noise sources can be on the same order as or larger than the shot-noise deviations, even though they would have been fairly insignificant compared to ambient scattering.

3. MODELING OF SCATTERING IN THE SHORT WAVELENGTH REGIME

Optical and X-ray systems use photons to interrogate the surface. Models like DDSURF and EMFLEX have been used for several years to calculate the scattering from particles and defects in the visible wavelength regime. X-ray scattering though is quite different from the former regime for several reasons. At sufficiently short wavelengths diffraction effects due to the arrangement of the atoms in the solid become significant, so the assumption that the solid is a continuum used in modeling scattering at longer wavelengths may no longer be valid. Short wavelength optical properties can also be quite different. Sub-unity refractive indices are the norm and they can be surprisingly small fractions near absorption peaks. Also, the assumption of small-particle optical properties from bulk optical properties has been a perennial concern at visible wavelengths, and the concern certainly is not lessened at short wavelengths where even the bulk materials are not as well characterized.

An important consequence is that, whereas in the visible-UV range nanoparticle scattering tends to increase with decreasing wavelength, in the X-ray regime ($\lambda < 10$ nm), the opposite trend holds.[7] Particle scattering can usually be expected to peak for wavelengths on the order or within a few orders of the particle diameter. The photon fluxes from most contemporary X-ray sources excluding synchrotrons (which are very expensive) is typically five or six orders of magnitude less than that available from visible-UV laser sources. Based on the above two observations, we should really be considering X-ray illumination very close to the extreme UV (EUV, 10 - 100 nm) where the scattering has not started to decrease to a large extent. Shorter wavelengths would combine weaker sources with reduced cross sections, which can hardly recommend them.

The usefulness of the EUV/X-ray transitional region needs to be explored further. Few scattering models have been validated at these transitional wavelengths between the X-ray and the visible-UV regime. However, it is expected that, while the scattering will probably peak in this transitional wavelength range, the scattering cross-sections will probably show strong oscillations due to wavelength resonances. We performed scattering calculations in the ultraviolet wavelength range for a 60 nm polystyrene latex (PSL) sphere on a bare wafer using DDSURF, as shown in Figure 3. The oscillatory behavior of the scattering cross section appears somewhat indistinct in this case, though it does appear more strongly in other cases and the wide spacing between wavelengths undoubtedly obscures it to some degree. There is a distinct maximum at 90 nm in the scattering cross section as a function of wavelength. The position of the global maximum for the scattering is a function of

particle size, shape and composition. Due to this variability and the existence of local maxima, simply using the wavelength for the global maximum would complicate reliable detection since, for example, a 21 nm particle might show a very high cross-section at a particular wavelength, while a 30 nm particle might show an unexpectedly low one.

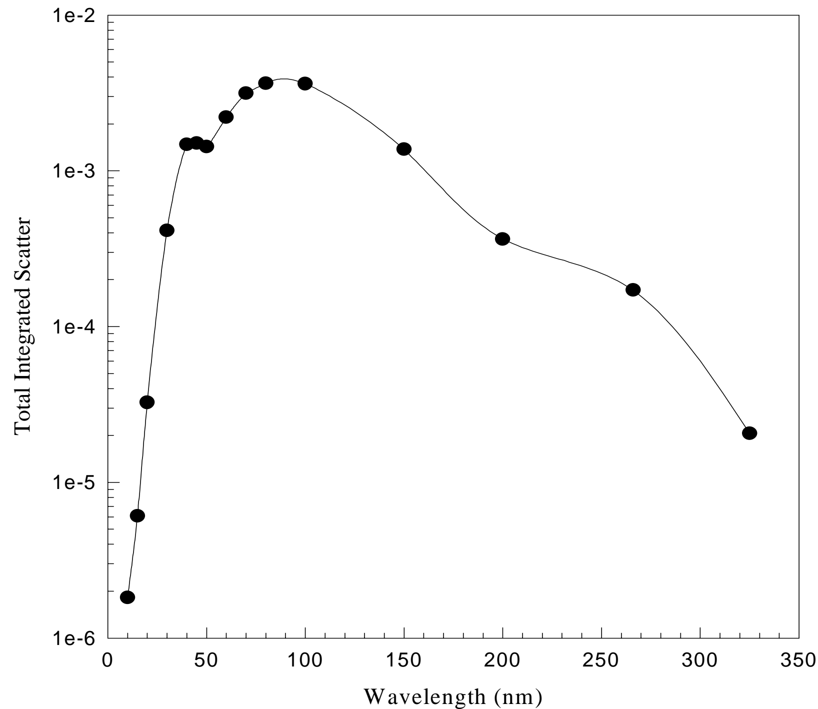

Figure 3. Scattering cross section as a function of wavelength for a 60 nm polystyrene latex particle on silicon wafer.

These considerations make it likely that we would want to avoid illumination wavelengths where the resonance phenomenon might occur for the expected types of particles, particularly if we intend to extract size information beyond a simple binning of particles greater than a certain PSL-equivalent size. Obviously, going to a wavelength such that it is just less than the low side of where the smallest particle of interest begins to show oscillations would increase the likelihood that larger particles will not show oscillations either. This argues for shorter wavelengths, but the scattering cross sections for a particle might be so small at that point as to be below the detection limit.

Figure 4 shows the plot of C_P *vs*. C_B for the data from Fig. 3, using the 300 mm wafer/min scan speed and other parameters identical to those in Fig. 2, except for the incidence angle. This plot similarly uses scatter by 0.1 nm RMS roughness as the background limitation, though the realism of this background model is somewhat questionable. The oscillations in the curve are less visible in this presentation, but the optimal wavelength range for this particle using this hypothetical apparatus is clear.

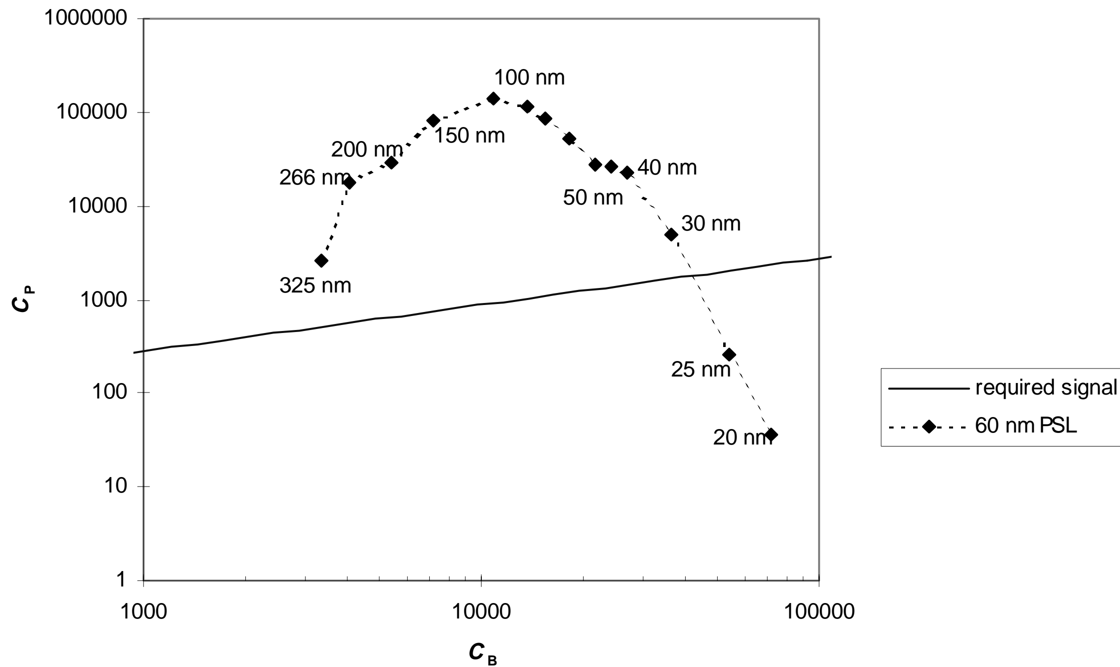

Figure 4. The signal count *vs.* background count as a function of wavelength for a 60 nm polystyrene particle on a silicon wafer with 0.1 nm RMS roughness.

Current optical wafer scanners also must face the problem of wavelength-resonance oscillations as well, but their detection limit sizes are usually much smaller than their illumination wavelengths. This situation can work for simple detection because the troughs in the oscillatory region can still have cross-sections higher than the cross-sections at the detection limit if the detection limit size is sufficiently less than the size range where the oscillations occur. Any sub-threshold troughs may also cover only a small range of sizes and so might then cause only a negligible rate of missed particles. Of course, in any case this complicates particle sizing to a large degree.

More work is currently being performed under our follow-up research contract to characterize scattering in the transitional EUV/X-ray region and to determine where the oscillations for nanoparticles begin and end, how high and low the oscillations go, and how the cross-sections on either side of the oscillatory region compare. Further work will be performed to calculate the scattering over the wavelength range as a function of particle size, and to determine whether there is any particular wavelength regime before the resonance phenomena begins where the scattering for all particle sizes is in the detectable region.

Considering that the transitional region is expected to be of interest, current numerical scattering codes might be need to be modified to account for atomic granularity. The approximations typically used in models of X-ray scattering probably cannot be relied upon in this regime either.

4. EXPERIMENTAL ASPECTS OF PARTICLE DETECTION IN SHORT WAVELENGTH RADIATION

We can identify three main groups of components for a short-wavelength optical scanning system capable of detecting nanoparticles on wafer surfaces, the radiation source, the optics, and the detectors, of which we will now address the

first two. Besides the design limitations imposed by high speed scanning, the interplay between the optics design and the choice of the radiation source will determine the feasibility of performing experiments in the short ultraviolet regime.

4.1 Radiation sources

The most important parameters for the selection of a short wavelength radiation source are wavelength, photon flux, cost, stability, and size of source. Neither particularly narrow linewidth nor coherence is essential. Lasers are used almost exclusively in visible-wavelength systems mainly because of their brightness (high flux density) and stability, so it is important not to allow this visible-wavelength prejudice to cause us to overlook the possibilities of broad-line incoherent UV sources, particularly since far-UV lasers are rather non-ideal in many respects.

In fact, no currently existing sources can really be considered ideal. Below, some of the possible sources in the ultraviolet and X-ray regimes are discussed. It should be noted as well that considerable research is being conducted into developing radiation sources capable of meeting the requirements for X-ray/EUV lithography systems. This research will undoubtedly lead to a number of improvements which will benefit X-ray/UV inspection and analytical technologies.

4.1.1 Ultraviolet lasers

A number of laser technologies have pushed into the ultraviolet so we naturally should examine these traditional sources first. Excimer lasers are available at wavelengths as short as 157 nm (F_2) with average fluxes at least comparable to the lasers illuminating visible-wavelength systems. However, such lasers are usually pulsed rather than CW, which introduces some complications into the system design. Excimer lasers are also somewhat expensive and can be difficult to operate in a number of ways.

Quite a variety of lasers can operate in the 200-300 nm range, both pulsed excimer systems and CW frequency-doubled ion systems. CW systems of sufficient power ($\geq$100 mW) are commercially available at as short as 229 nm.

It is probably safe to assume that, particularly five or ten years from now, there will be no difficulty in obtaining UV lasers suitable for an inspection system at wavelengths above 150 nm. Consequently, we need only concern ourselves with more exotic sources at shorter wavelengths.

4.1.2 Synchrotron radiation sources

Synchrotron radiation has the important characteristics of high brightness (high flux per unit area per solid angle), tunability, and coherence. Synchrotrons are the in fact the brightest practical (in a manner of speaking) source of extreme ultraviolet and X-ray radiation, however they have significant disadvantages in cost, size, and complexity. The range of wavelengths available by tuning is also relatively restricted in the EUV.

Much current research in synchrotron development is aimed toward compact synchrotron sources for applications in industry. In contrast to the today's research-oriented synchrotron sources where brightness is the key design goal, the compact rings are designed along guidelines of size, cost efficiency, reliability, and compatibility with an industrial environment. Research is also being conducted towards developing the related technology of free electron lasers[8] (FELs) as X-ray sources. Such sources could produce short-wavelength radiation brighter than synchrotron sources.

4.1.3 Laser-produced plasma sources

Laser produced plasmas are one of the potential alternatives for generating extreme ultraviolet radiation in the laboratory. A high intensity pulse (10^{14} -10^{17} W/cm^2) of focused long-wavelength laser radiation is shone on a target surface to create a plasma. The conversion of a significant proportion of the incident laser energy to ultraviolet radiation can be obtained. Laser produced plasmas are being considered as potential alternative for extreme ultraviolet lithography, but the technology has problems associated with debris from that target surface and a low repetition rate.

4.1.4 Ultraviolet lamps

A number of other incoherent extreme ultraviolet and X-ray sources have been in use for some time. The best-known of these rely on electronic transitions within excited atoms and molecules. The problem of producing radiation from a given atom or ion essentially becomes the problem of creating the excited atom or ion, and various excitation mechanisms have been used such as DC glow discharge or more energetic spark discharge. Samson[9] gives a comprehensive description of the various ultraviolet sources, some of the important being the, hydrogen glow discharge lamp, Lyman continuum and Penang discharge lamp[10] (using rare gases). A high flux of radiation is obtainable from ultraviolet lamps, but the flux must then be concentrated considerably to achieve high brightness. Ultraviolet lamps tend to have low durability (cathode erosion), produce incoherent radiation, and have low spectral resolution, but only the durability and brightness issues are a significant drawbacks for particle detection applications.

4.2 Short wavelength optics

In the extreme ultraviolet regime many of the bulk materials which are transparent in the visible region are opaque. The absence of sufficiently transparent material in the extreme ultraviolet has led to the ever growing use of reflective optics for focusing and deflecting beams. Two important kinds of reflectors are the grazing incidence mirrors and multilayer coatings (Bragg stacks).

The refractive indices of all materials are very close to 1 in the extreme ultraviolet to the X-ray region. Reflection can only be obtained at large angles of incidence where the rays make a small angle with the mirror surface (grazing). Due to the small grazing angle of incidence the optics design in the extreme ultraviolet and X-ray region is much different from that in conventional optics. The reflectivity of single mirror surfaces at grazing angles greater than the critical angle is very small. This will pose a problem in the design of a optical system using short wavelength radiation for particle detection on silicon wafer surface. To ensure a high reflectivity at the silicon surface the radiation needs to be incident at a small grazing angle, leading to a lower flux density at the surface (due to increase in the beam width). The flux density is important in determining the scattering signal obtained from the particle.

The reflectivity in the extreme ultraviolet region can be improved by using multilayer coatings. Multilayer coatings are stacks of ultrathin films of alternately high and low refractive indices. Gullikson[11] *et al.* have obtained a reflectivity of 65% for multilayer coating of Mo/Si layers at normal incidence of synchrotron radiation with a wavelength of 13.4 nm. The reflectivities obtained for multilayer coatings are wavelength specific, so they cannot achieve high reflectivities over a wide entire wavelength band. The radiation source should be capable of generating high flux in the narrow window of wavelength in the extreme ultraviolet region where the reflectivity of the optics is high. Another problem is the reduced performance of these coatings due to interfacial roughness. High flux densities can heat the coatings and degrade the performance of the mirror.

The interplay between the optics and the choice of the radiation source is important. Synchrotron radiation is the brightest source of extreme ultraviolet and X-ray radiation. An important benefit of high brightness is the ability to obtain high spatial resolution. With the help of special optical devices such as a Fresnel zone plate, spot sizes as small as 30 nm can be obtained. The small spot size could be beneficial in overcoming the decrease in the flux density at the surface due to the use of a grazing angle of incidence. The high spectral resolution and tunable nature of the synchrotron radiation will be useful in obtaining radiation in a narrow wavelength window.

5. CONCLUSIONS

The continuing reduction in the dimensions of the structures manufactured on wafer surfaces requires the ability to detect and identify contaminants of ever smaller dimensions, as delineated in the National Technology Roadmap for Semiconductors. Conventional visible wavelength inspection techniques will not be able to meet these requirements, so in the context of this concern we at ASU have addressed the issue of alternative particle detection techniques. In the present work we have examined the feasibility of using short wavelength radiation as an alternative particle detection technique.

Using our presented methodology for the analysis of high-speed detection performance, we can say that there is a good probability of success using short wavelength radiation in the extreme ultraviolet regime (less than 100 nm), but this is not a certainty. Longer ultraviolet wavelengths offer more doubtful prospects but should not be discounted at this point, and

shorter X-ray wavelengths are even less probable due to a current dearth of suitable sources as well as a downward trend in scattering cross section as wavelength decreases past a certain point.

However, a number of issues are still be settled, including the questions as to the dominant background source and its magnitude in hypothetical low-pressure short-wavelength surface inspection systems. Better characterization of particle scattering in the EUV range is also needed and is presently under way.

We have also seen that ongoing research into UV and X-ray technology, especially related to the development of EUV lithography, is providing an impetus for the development of better UV and X-ray sources (e.g. compact synchrotrons, free-electron lasers) and more efficient optics.

6. ACKNOWLEDGEMENTS

This work was supported by the Semiconductor Research Corporation.

7. REFERENCES

[1] Semiconductor Industry Association, *National Technology Roadmap for Semiconductors,* Sematech Inc., 1997.
[2] B.D. Buckner, *A Model For The Performance Of Surface-Scanning Inspection Systems*, M.S. Thesis, Dept. of Electrical Engineering, Arizona State University, 1996. (see http://enws347.eas.asu.edu/~buckner/msthesis.pdf)
[3] J.M. Elson, J.P. Rahn, J.M. Bennett, "Relationship of the Total Integrated Scattering from Multilayer-coated Optics to Angle of Incidence, Polarization, Correlation Length, and Roughness Cross-Correlation Properties," Appl. Opt. **20**, pp. 3207-3219, 1983.
[4] B.M. Nebeker, G.W. Starr, and E.D. Hirleman, "Modeling of light scattering from structures with particle contaminants," in *Flatness, Roughness, and Discrete Defect Characterization for Computer Disks, Wafers, and Flat Panel Displays*, John Stover, ed., Proc. SPIE **2862**, pp. 139-150, 1996.
[5] R.L. McKenzie, "A Method of Atmospheric Density Measurements During Space Shuttle Entry Using Ultraviolet-Laser Rayleigh Scattering," NASA Technical Memorandum 100056, NASA Ames Research Center, 1988.
[6] R. Penndorf, "Tables of the Refractive Index for Standard Air and the Rayleigh Scattering Coefficient for the Spectral Region between 0.2 and 20.0 μ and Their Application to Atmospheric Optics," J. Opt. Soc. Am. **47**, pp. 176-182, 1957.
[7] J.R.H. Herring, “Grazing Incidence X-ray Scattering Evaluation of Polished Surface Quality, and Associated Instrumental and Residual Particle Effects,” Applied Optics **23**, pp. 1156-1165, 1984.
[8] I.H. Winick, *Synchrotron Radiation Sources - A Primer*, pp. 13-15, World Scientific Publishing Co. Pte. Ltd.: River Edge, NJ, 1994.
[9] S. Bowyer, “Continuous Emission Source Covering the 50-300 Å Band,” Applied Optics **32,** pp. 6930-33, 1993.
[10] J.A.R. Samson, *Techniques of Vacuum Ultraviolet Spectroscopy,* Wiley & Sons Inc.: New York, 1967
[11] E.M. Gullikson, D.G. Stearns, D.P. Gaines, and J.H. Underwood, “Non-specular scattering from multilayer mirrors at normal incidence” in *Grazing Incidence and Multilayer X-ray Optical Systems*, R.B. Hoover and A. B. C. Walker II, eds., Proc. SPIE **3113**, pp. 412-419, 1997.